Academic Journal of Science and Technology
ISSN: 2771-3032 | Vol. 5, No. 2, 2023

Numerical Simulation Study of Static Fracture Technology of Borehole with Prefabricated Fracture

Gaoyu Cheng[1, *], Zhiqiang Hou[1], Mengzhuo Li[1]

[1]Henan Polytechnic University, Jiaozuo 454003, China

[*] **Corresponding author**: 212002020021@home.hpu.edu.cn

Abstract: Because of the danger of blasting to local underground rock-breaking engineering, the construction under complex environment is realized by using prefabricated crack drilling and static crushing technology. In order to predict the crushing effect, based on the cohesion element method, different hole spacing, prefabricated fissure length and surrounding rock are selected to carry out the numerical simulation study of static crushing prefabricated fissure borehole, the prediction models of fracture pressure and initiation pressure are established.

Keywords: Prefabricated fracture, Static cracker agent, Crack propagation.

1. Introduction

For underground rock engineering, blasting or mechanical rock breaking is often used. Although these two methods can crack rock, the problems of shock wave, vibration, dusty, toxic gases of blasting, serious wear of mechanical rock-breaking equipment have seriously affected the construction efficiency. It is not suitable for underground rock breaking construction, so the static breaking technology is produced. The static crushing technology fills the static crushing agent slurry into the drilling hole of the broken material, and the volume expansion occurs through the hydration reaction, and the expansion pressure is produced, which causes the medium to break, the utility model has the advantages of no open fire, no vibration, stable performance, easy operation [1-3]. With the requirement of ecology, environment protection and safety in the construction process, and the restriction of blasting materials in some special circumstances, the static crushing technology is widely used in engineering.

However, in the construction of large-scale compact hard rock, due to the limited expansion pressure of static breaker and uniform bearing pressure on the wall of circular borehole, the cracking pressure is relatively large. Therefore, pre-cutting the borehole wall to form prefabricated fracture and form local stress concentration can effectively control the direction of crack propagation and reduce the pressure demand of crack initiation. Meanwhile, the effect and efficiency of fracturing can be greatly improved by simultaneously arranging several boreholes to form a fracturing network. Therefore, it is very significant to study the fracturing of rock with prefabricated fractures in actual construction.

The study of crack is based on single crack model. Inglis proves the existence of tip stress concentration by calculating the stress distribution of plate with elliptical hole under the action of tensile stress, in a follow-up study, middle-aged men came up with the concept of Stress intensity factor, which became the basis of fracture criterion [4]. Griffith calculated the stress distribution based on Inglis by solving the elastic potential energy released by the elastic plate by integral method, and carried out experimental research using glass and ceramic materials, and obtained the Griffith Energy criterion based on energy for crack propagation [5]. Orowan then modified the Griffith energy criterion by further study [6]. From 1961 to 1986, Wells and Rice put forward the concepts of crack tip opening displacement criterion and J integral respectively, and applied them to the criterion of crack initiation [7-8]. Erdogan and Sih put forward the theory of maximum axial tensile stress by taking the maximum circumferential tensile stress as the cause of cracking, and considered that the crack will propagate along the direction of the maximum circumferential tensile stress after cracking [9]. Hussain et al through the study of composite fractures, used the energy release rate as a criterion for judging the initiation of cracks, namely the maximum energy release rate theory, and considered that cracks would propagate along the direction of the maximum energy release rate at the tip. Sih puts forward s criterion, which takes strain energy density factor as an index to judge the crack initiation and propagation direction [10]. Since then, many other fracture criteria have been proposed on the basis of these three classical fracture criteria [11].

The common methods of crack simulation include solid element deletion method [12], the extended finite element method (XFEM) [13], the virtual crack closure technique (VCCT) [14], cohesion element method [15], the discrete element method (DEM) [16]. However, the above-mentioned methods have some defects in the simulation of rock crack propagation. The solid element deletion method cannot simulate the contact slip between cracks because the element is deleted by setting the strength rule. XFEM can simulate the fatigue fracture of materials by inserting the initial crack, but its algorithm does not allow the crack to cross and cannot simulate the random propagation of rock crack. However, the cohesive force element method can set the nonlinear damage zone at the crack tip, avoid the stress singularity at the crack tip, and simulate the complex contact and interaction between cracks.

This paper aims to investigate the characteristics of rock crack propagation are studied under the conditions of different pore arrangement parameters. As shown in Figure 1, due to the presence of in-situ stress in underground construction, the effect of vertical stress is also considered in this study. The research results are of great significance to the propagation and mechanism of static induced crack in underground rock mass.

2. Simulation Method of Rock Crack Propagation

(1) Cohesion element method

A Cohesive Element used to deal with problems such as Cohesive structures, material interfaces, and rock fracture. The thickness of cohesive element is nearly zero, so it can be embedded between solid elements flexibly, and the damage caused by external force can be limited to the cohesive element, while other elements are not affected. The crack initiation and propagation can be regarded as a gradual separation process between the cohesive element and the traditional solid element when the cohesive element is used to simulate the crack propagation.

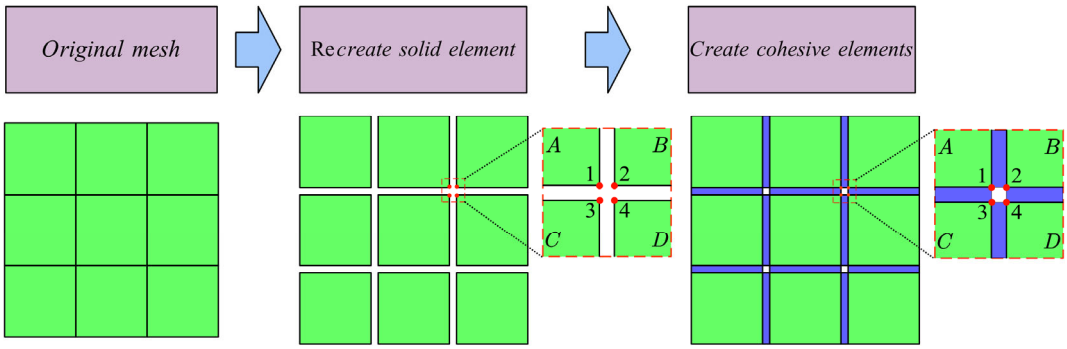

Figure 1. Process of generating zero-thickness cohesive elements at every solid element interface

Fig.1 shows the process of generating a zero-thickness cohesion element in a solid element. The model consists of solid elements (green) and cohesion elements (blue). The algorithm used is written in Python, the cohesion element is generated by reading and modifying the model file. According to the modeling principle of the cohesive force model, the generation and propagation of crack are affected by the solid grid when the crack is simulated by this method, the grid should be divided into irregular grids.

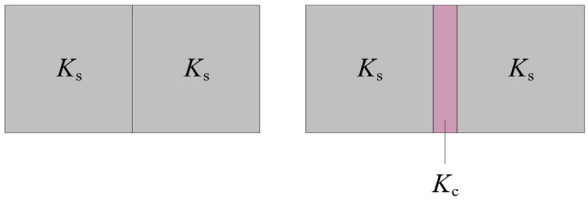

Figure 2. Diagram of stiffness calculation of connecting element

As shown in Fig.2. When two solid elements are in series, their total stiffness K_0 can be calculated by

$$K_0 = \frac{1}{(1/K_s) + (1/K_s)} = \frac{K_s}{2} \tag{1}$$

where K_s is the initial stiffness of the solid element.

When a cohesive element is inserted between two solid elements,, the new total stiffness K_s' can be calculated by

$$K_0^{'} = \frac{1}{(1/K_s) + (1/K_s) + (1/K_c)} = \frac{K_s}{2 + (K_s/K_c)} \tag{2}$$

Where K_c is the initial stiffness of the cohesive element.

According to equation (2) and (2), the total stiffness is reduced because of inserting cohesive element. In order to avoid this affect, K_c should be much greater than K_s.

(2) Traction-separation law

When crack propagation is carried out with cohesive element, the damage of cohesive element is usually described by the traction-separation law. Fig.3 is a typical traction-separation law response. The crack initiation and propagation are considered to be caused by the traction force between the top and bottom surfaces of the cohesive element. In the two-dimensional model, the traction force includes the tensile stress and the shear stress. In this study, the tensile stress and the tensile strain are considered as positive values, and the compressive stress and the compressive displacement are considered as negative values. When the traction force is greater than the set strength of the material, the cohesion element begins to be damaged, and its stiffness decreases with the increase of the separation displacement of the element, and when the element is completely damaged, it shows that the cohesion element is completely invalid, the crack propagates forward. In the simulation of crack growth, the traction separation law can be divided into three stages: linear elastic stage (OA) , damage initiation stage (A) and damage evolution stage (AB).

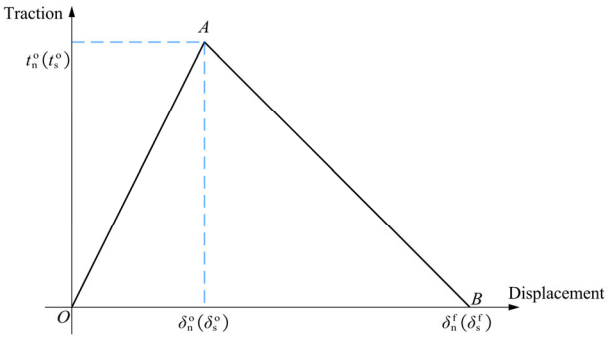

Figure 3. Typical traction-separation response

Linear elastic stage (OA). n the two-dimensional model, the traction force can be divided into normal traction t_n and shear traction t_s. the elastic relationship can be represented as

$$t = \begin{bmatrix} t_n \\ t_s \end{bmatrix} = \begin{bmatrix} K_{nn} & K_{nt} \\ K_{nt} & K_{tt} \end{bmatrix} \begin{bmatrix} \delta_n \\ \delta_s \end{bmatrix} = K\delta \tag{3}$$

Where the K is the stiffness matrix of the element.

Damage initiation stage (A). When t_n <0, the damage of cohesive elements is caused by compressive stress which can be assumed to obey the Mohr-Coulomb criterion. When $t_n \geq 0$, the damage of cohesive elements begins when the nominal

stress ratios in the quadratic interaction function below reaches 1. The criterion is represented as

$$\begin{cases} |t_s| = S - t_n \tan\phi, & t_n < 0 \\ \left(\dfrac{\langle t_n \rangle}{T}\right)^2 + \left(\dfrac{t_s}{S}\right)^2 = 1, & t_n \geq 0 \end{cases} \tag{4}$$

Where the T is the tensile strength of cohesive elements.

Damage evolution stage (AB). In this stage, the stiffness of the cohesive element will be decrease with the increase of the separation displacement. The damage variable D represent all damage of cohesive element. The initial value of D is zero and evolve to 1 with the traction force increasing. The evolution can be described as

$$\begin{cases} t_n = \begin{cases} (1-D)\,\bar{t}_n, & t_n \geq 0 \\ \bar{t}_n, & t_n < 0 \end{cases} \\ t_s = (1-D)\,\bar{t}_s \end{cases} \tag{5}$$

3. Numerical Simulation Process

(1) The mechanical parameter and expansion pressure curve

In this study, using C50 concrete parameter which obtain the required mechanical properties by uniaxial compression and Brazilian splitting tests, as shown in Table 1.

Table 1. Table of rock parameters for numerical simulation

Mechanical parameter	Values
Elastic modulus (GPa)	37.2
Poisson's ratio	0.2
Cohesion of the solid element (MPa)	16.3
Friction angle (°)	33
Tensile strength, (MPa)	3.67
Fracture energy (Pa·m)	12.25

According to the standard test method, the static pressure curve of the crusher was obtained under laboratory conditions. The pressure curve can be divided into three stages: initial stage, rapid expansion stage and slow expansion stage. The maximum expansion pressure was 65.8mpa, and since the monitoring data fluctuated within a small range, the curve was fitted with Python, with a goodness of fit of 99.98%.

(2) Test schemes

According to previous research, rock crack propagation is affected by many factors. In this study, the initiation and propagation of SCA-induced crack in rock are studied by setting different hole spacing (L), prefabricated crack length (a) and confining pressure (σ). The value of those three factor is shown in Tab.2.

Table 2. Numerical simulation drill hole layout parameter table

	I	II	III
L/mm	700	1000	
a/mm	30	50	100
σ/MPa	4	8	

4. Analysis of Numerical Simulation Results

(1) Crack characteristics

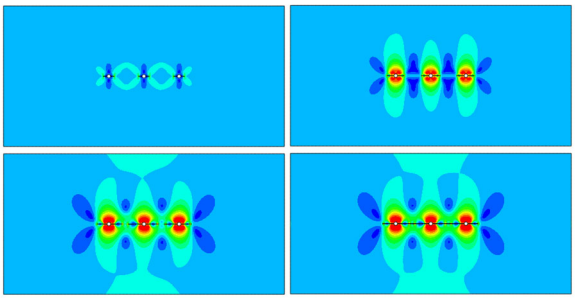

Figure 4. Numerical simulation results

Fig 4 shows the four stages of crack propagation, including initiation, crack initiation, crack propagation and crack penetration. In the initial stage of fracturing, the static breaking agent is in the reaction stage, and almost has no expansion pressure. Due to confining pressure, there will be some stress concentration around the tip of borehole and prefabricated fracture The tensile stress at the tip of the precast crack increases with the increase of the expansion pressure in the hole. When the stress concentration reaches the failure condition of the material, the precast crack tip begins to crack, with the increase of the expansion pressure, the crack began to expand. Because of the free surface between the boreholes, the crack basically propagated along the borehole line until the two cracks penetrated.

(2) Effect of prefabricated fracture length and confining pressure on initiation pressure P_0.

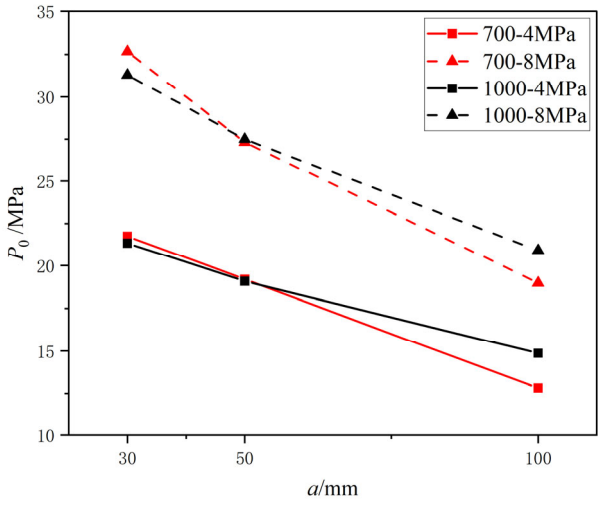

Figure 5. Initiation pressure of prefabricated fracture

Because of the stress concentration at the crack tip, the crack initiation pressure is an important index to evaluate rock fracture. The bigger the crack initiation pressure is, the more difficult the rock fracture is. Figure 5 shows the expansion pressure at the beginning of the precast crack in a numerical simulation test. The results show that the initiation pressure decreases with the increase of the length of the precast crack and increases with the increase of confining pressure

Tade et al have studied and summarized the method for calculating the mode I Stress intensity factor at the crack tip of a symmetric crack in an infinite plate under internal pressure in a circular hole, as shown, by using the boundary collocation method [17]. The expression is as follows:

$$\begin{cases} K_1 = P\sqrt{\pi a}\, F_\lambda(s) \\ F_\lambda(s) = (1-\lambda)F_0(s) + \lambda F_1(s) \\ F_0(s) = (1-s)\left[0.637 + 0.485(1-s)^2 + 0.4s^2(1-s)\right] \\ F_1(s) = 1 + (1-s)\left[0.5 + 0.743(1-s)^2\right] \end{cases} \quad (6)$$

where λ is the fracture pressure coefficient, $s = a/(a+R)$; R is the radius of round hole, mm; a is the length of precast fracture.

When the prefabricated fissures pressure coefficient λ=1, the influence of confining pressure on initiation pressure is taken into account, the constant term of the formula is modified by Python function fitting, as shown in Equation (7).

$$P_0 = \frac{K_I}{P\sqrt{\pi a}\left(1 + (1-s)\left[0.25 - 0.740(1-s)^2\right]\right)} + \frac{1.17}{R}\sigma \quad (7)$$

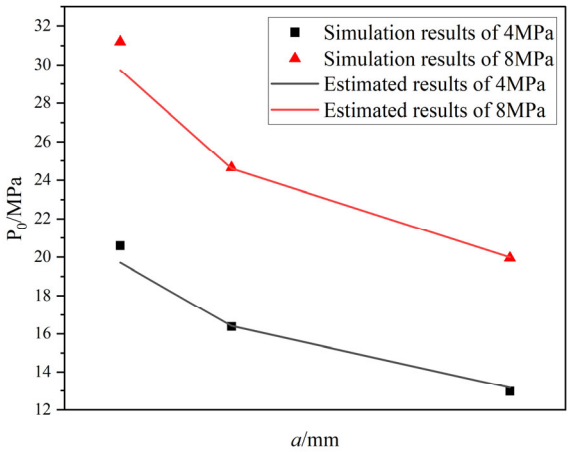

Figure 6. Test of predictive equation

The test parameters were tested by Equation(7), as shown in Figure6, in which the maximum error value was 1.58 MPa, the minimum value was 0.05 MPA, the average difference value was 0.98 MPA, the error range was 2% ~ 11%, the average value was 3.2% , the error values are all within the acceptable range.

(3) Fracture pressure (P_{ex}) prediction equation

Fig 7 shows the fracture pressure in the hole when the crack penetrates between the holes under different parameters. It can be seen from Fig.7 that: other conditions are the same, the through pressure increases with the increase of hole spacing and confining pressure, and decreases with the increase of precast fracture length.

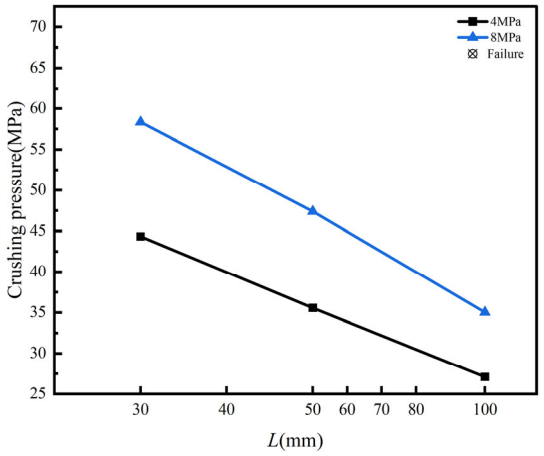

(b) *L*=700mm

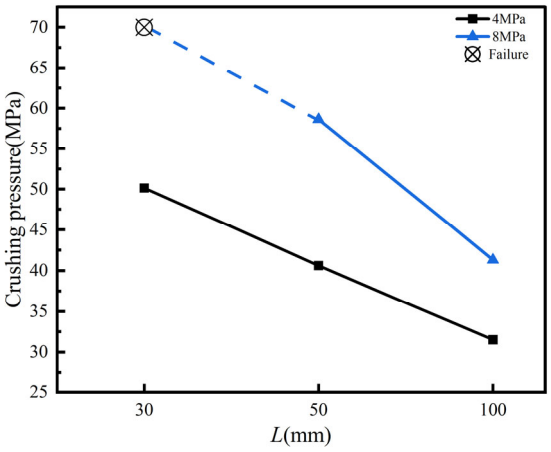

(c) *L*=1000mm

Figure 7. The effect of L and a on crushing pressure

Based on the through pressure obtained by numerical simulation, the predictive equations relating to the through pressure and hole spacing, prefabricated fracture length and confining pressure are obtained by data fitting, as shown in Equation (8).

$$P_{ex} \geqslant \frac{K_{IC}}{\sqrt{\pi a}\left(\frac{0.3}{a} - 0.0557\right)} \times \left(\frac{0.34}{a} + 2.24\right) \times 10^{-3} \times \frac{\frac{L}{2} + R}{2R^2} \quad (8)$$

The maximum difference between the predicted value and the simulated data calculated by Equation (14) is 3.56 MPa, the minimum difference is 0.025 MPa, the average difference is 0.968 MPa, and the difference is within the acceptable range.

5. Conclusion

In order to improve the effect of SCA on rock cracking, the crack initiation and propagation under different hole spacing, prefabricated crack length and confining pressure are simulated by using cohesive element method, based on the previous theoretical research, the prediction equations of fracture pressure and breakthrough pressure are summarized:

(1) The initiation pressure P_0 can be used as an effective index to evaluate the difficulty of rock fracturing. For the

rocks with high initiation pressure, the initiation pressure can be reduced by increasing the length of the prefabricated fracture, so as to improve the fracturing effect. The prediction formula for the initiation pressure is

$$P_0 = \frac{K_I}{P\sqrt{\pi a}\left(1+(1-s)\left[0.25-0.740(1-s)^2\right]\right)} + \frac{1.17}{R}\sigma \quad (9)$$

(2) Basing on the analysis of the hole distribution parameters, it is shown that the hole spacing, the length of the prefabricated crack and the confining pressure affect the inter hole penetrating pressure: with the increase of the hole spacing, the edge length of the crack growth length is longer, a larger fracture pressure is required to form an influence zone to promote crack growth; at the same expansion pressure, a crack can be formed at the tip of the prefabricated crack, thus promoting faster crack growth and thus reducing the demand for expansion pressure. The prediction formula for the through pressure is

$$P_{ex} \geqslant \frac{K_{IC}}{\sqrt{\pi a}\left(\frac{0.3}{a}-0.0557\right)} \times\left(\frac{0.34}{a}+2.24\right)\times 10^{-3}\times\frac{\frac{L}{2}+R}{2R^2} \quad (10)$$

(3) In actual construction, the physical and mechanical parameters of in-situ rock stress and fracturing rock can be obtained by field test and laboratory test, and the cracking pressure and fracture pressure can be predicted by the formula, the expansion pressure for fracturing the rock is calculated by choosing suitable hole spacing and prefabricated fracture length, and is verified by numerical simulation based on the selected parameters.

References

[1] Zhang Chao, Lin Baiquan, Zhou Yan, et al. Deep-hole directional static cracking technique for pressure relief and permeability improvement in mining-coal bed [J]. Journal of Mining & Safety Engineering, 2013,30(04):600-604.

[2] Zhang Chao, Lin Baiquan, Zhou Yan, et al. Application of multi-seam metal jet directed pre-split blasting technology in gas extraction [J].Journal of China Coal Society, 2014, 39 (S1):100-104.

[3] Huynh M P, Laefer D F. Expansive cements and soundless chemical demolition agents : state of technology review: The 11th Conference on Science and Technology[C], 2009.

[4] R. I G. Analysis of Stresses and Strains Near the End of a Crack Traversing a Plate[J]. J. Appl. Mech, 1957,24(3).

[5] Griffith A A. The Phenomena of Rupture and Flow in Solids[J]. Philosophical Transactions of the Royal Society of London. Series A, Containing Papers of a Mathematical or Physical Character, 1921,221.

[6] Orowan E. Fracture and strength of solids[J]. Reports on Progress in Physics, 1949,12(1).

[7] Wells A A. Application of fracture mechanics at and beyond general yield[J]. 1963.

[8] Rice J R. A Path Independent Integral and the Approximate Analysis of Strain Concentration by Notches and Cracks[J]. Journal of Applied Mechanics, 1968,35(2):379-386.

[9] Erdoga F. On the Crack Extension in Plates Under Plane Loading and Transverse Shear[J]. J Basic Eng, 1963,12.

[10] Sih G C. Strain-energy-density factor applied to mixed mode crack problems[J]. International Journal of Fracture, 1974,10(3).

[11] Hussain M A, Pu S L, Underwood J H. Strain Energy Release Rate for a Crack Under Combined Mode I and Mode II[J]. Strain Energy Release Rate for A Crack Under Combined Mode I & Mode II, 1973.

[12] G. Li and C. A. Tang. A statistical meso-damage mechanical method for modeling trans-scale progressive failure process of rock [J]. International Journal of Rock Mechanics and Mining Sciences, 2015, 74:133–150.

[13] E. Mikaeili and P. F. Liu. Numerical modeling of shear band propagation in porous plastic dilatant materials by XFEM [J]. Georetical and Applied Fracture Mechanics, 2018, 95:164–176.

[14] M. M. Shokrieh, H. Rajabpour-Shirazi, M. Heidari-Rarani, and M. Haghpanahi .Simulation of mode I delamination propagation in multidirectional composites with R-curve effects using VCCT method [J]. Computational Materials Science, 2012,65:66–73.

[15] A. Tabiei and W. L. Zhang. Cohesive element approach for dynamic crack propagation: artificial compliance and mesh dependency [J]. Engineering Fracture Mechanics, 2017, 180: 23–42.

[16] L. Chuang, L. Huamin, and J. Dongjie. Numerical simulation study on the relationship between mining heights and shield resistance in longwall panel [J]. International Journal of Mining Science and Technology, 2017, 27,2,: 293–297.

[17] Tada. The stress analysis of cracks handbook[M]. ASME Press, 2000.